Nonlinear Dyn (2021) 103:1955–1967
https://doi.org/10.1007/s11071-020-06183-4

ORIGINAL PAPER

Strong chaotification and robust chaos in the Duffing oscillator induced by two-frequency excitation

André Gusso · **Sebastian Ujevic** · **Ricardo L. Viana**

Received: 20 May 2020 / Accepted: 29 December 2020 / Published online: 12 February 2021

Abstract In this work, we demonstrate numerically that two-frequency excitation is an effective method to produce chaotification over very large regions of the parameter space for the Duffing oscillator with single- and double-well potentials. It is also shown that chaos is robust in the last case. Robust chaos is characterized by the existence of a single chaotic attractor which is not altered by changes in the system parameters. It is generally required for practical applications of chaos to prevent the effects of fabrication tolerances, external influences, and aging that can destroy chaos. After showing that very large and continuous regions in the parameter space develop a chaotic dynamics under two-frequency excitation for the double-well Duffing oscillator, we demonstrate that chaos is robust over these regions. The proof is based upon the observation of the monotonic changes in the statistical properties of the chaotic attractor when the system parameters are varied and by its uniqueness, demonstrated by changing the initial conditions. The effects of a second frequency in the single-well Duffing oscillator is also investigated. While a quite significant chaotification is observed, chaos is generally not robust in this case.

A. Gusso (✉) · S. Ujevic
Departamento de Ciências Exatas, Universidade Federal Fluminense, Volta Redonda, RJ 27255125, Brazil
e-mail: andregusso@id.uff.br

R. L. Viana
Departamento de Física, Universidade Federal do Paraná, Curitiba, PR 81531-980, Brazil

Keywords Duffing oscillator · Chaos · Chaotification · Robust Chaos

1 Introduction

Nonlinear dynamical systems are widely found in nature and engineering and have been investigated for both fundamental reasons and for their potential practical applications. One of the most interesting features of nonlinear systems is that in many cases they can develop chaos, the seemingly random behavior of the system which is, however, dictated by deterministic equations [1]. This chaotic dynamics is not only relevant for academic reasons, it is considered for practical applications. Examples are chaos-based communication [2], data encryption for secure communications [3], pseudo-random number generators [4,5], to improve the performance of switched mode power supplies [6], and in more efficient radars and sonars [7]. Some of these applications rely upon sources of continuous time chaotic signals, such as radars and certain communication systems, while others can also use a discontinuous source, like chaotic maps [8].

While many nonlinear dynamical systems may display chaos, it can be restricted to small regions in the parameter space, or be less complex than required for certain applications. In order to improve this condition, several methods for the chaotification of the dynamics have been developed [9]. These methods allowed to induce chaos even on linear systems, however, at

the cost of introducing relatively complex control systems. Here, we show that it is possible, in a very simple manner, to generate a strong chaotification (increased regions in the parameter space with chaos) in the Duffing oscillator, a well known and paradigmatic nonlinear system [10].

A potential problem for the practical applications based upon continuous chaotic signals generated by physical sources of chaos is that the known dynamical systems usually present fragile chaos. In this form of chaos, the chaotic attractor has other attractors in the vicinity of the parameter space. Therefore, small changes in the system parameters may change significantly its dynamics. This situation is nicely illustrated, for instance, by the phase diagrams for several relevant dynamical systems presented in [11]. If the chaotic attractor is fragile in a physical system designed as a source of chaotic signals, it may not develop the expected chaotic dynamics. This can be a result of imperfections in the fabrication process, which may produce a system with a set of parameters corresponding, for instance, to a nonchaotic attractor. Furthermore, even if the system starts by operating in a chaotic regime, it is possible that chaos disappears due to small changes in the operational parameters induced by external influences (vibrations, electromagnetic waves, heat, etc) or aging of the components. Such problems can be avoided in practical applications resorting to systems with robust chaos.

A concept first introduced by Banerjee et al. in [12], robust chaos is characterized by the existence of a single chaotic attractor which is not altered by changes in the system parameters. Banerjee et al. [12] first studied a chaotic map, and after their work, several other chaotic maps have been proven to have a robust chaotic attractor [8]. On the other hand, very few continuous time chaotic systems present the same characteristic [8]. Of particular relevance are the hyperbolic systems investigated by Kuznetsov et al. [13,14]. While based on well-established theoretical grounds, hyperbolic systems are hard to conceive as an actual physical system. However, Kuznetsov and collaborators have been able to devise adequate dynamical systems. They have proposed and investigated nonautonoumous nonlinear systems based on coupled oscillators, which have been implemented experimentally in the form of electronic circuits [13,14]. It was also recently discovered by Gusso et al. [15] that micro- and nanoresonators can display robust chaos. More specifically, they have found through an extensive numerical analysis that suspended beam micro- and nanoresonators when excited by two frequencies, through distinct lateral electrodes, can develop a large region with robust chaos. This finding is interesting because micro- and nanoresonators have been investigated for a large range of potential applications which include the generation of chaos [16,17], but in configurations for which only fragile chaos is expected. However, it was only recently that experiments have observed chaos in a microresonator of the kind investigated in Ref. [15] when excited by a single frequency [18], and further experimental investigations and characterization of the chaotic dynamics are needed.

In this work, we show through extensive numerical analysis that the Duffing oscillator [10] when excited by two frequencies develops robust chaos over very large regions in the relevant parameter space, like the nanoresonator in [15]. One of the motivations for this work is that each particular dynamical system has its advantages or limitations for a specific practical application, such as the maximum frequency of oscillation, spectral distribution of the chaotic signal, physical dimensions, power consumption, etc. Therefore, it is always necessary to have as many dynamical systems with robust chaos as possible to chose the one that fits better to a given application. Another motivation is to investigate whether other dynamical systems can develop robust chaos when excited by two frequencies.

The Duffing oscillator was chosen for several reasons. One is the mathematical similarity of Eq. (1) with the model describing the micro-/nanoresonators investigated by Gusso et al. [15]. Furthermore, there are several physical systems that can be described, at least approximately, by the Duffing equation. As an example, we have clamped beams excited by magnetomotive forces and used as micro- and nanoresonators [19]. In a one degree of freedom, reduced order (lumped mass) model of the beams a cubic, hardening type, nonlinear term results from the beam stretching effect [20]. Also, microelectromechanical oscillators of the spring-mass type investigated experimentally and displaying chaos were modeled using extensions of the Duffing equation [16,17]. Finally, the Duffing equation can be physically implemented by suitably designed mechanical and electronic systems. An interesting alternative of practical relevance is based upon simple electronic circuits [21], which can be designed within a large range of frequencies, power consumption, etc.

2 The Duffing oscillator

The Duffing oscillator is one of the simplest nonlinear oscillators and represents a simple extension of the harmonic oscillator. The equation for the driven Duffing oscillator has the form [10]

$$m\ddot{x} + c\dot{x} \pm kx + k_3x^3 = F(t), \tag{1}$$

where m represents the mass of the oscillating system, c the linear damping coefficient, k the linear spring constant, k_3 to the nonlinear spring constant. On the right-hand side of the equation, $F(t)$ represents a general forcing function. For a single harmonic forcing, $F(t) = A\cos(\omega t)$, Eq. (1) can be recast in a more convenient form, with the smallest number of free parameters. With the change of variables

$$s = k\frac{x}{A}, \quad \alpha = \frac{c}{\sqrt{k_1 m}}, \quad \beta = k_3\frac{A^2}{k^3}, \quad \omega_0 = \sqrt{\frac{k}{m}},$$

$$\tau = \omega_0 t, \quad \zeta = \frac{\omega}{\omega_0}, \tag{2}$$

Equation (1) turns into

$$\ddot{s} + \alpha\dot{s} \pm s + \beta s^3 = \cos(\zeta\tau), \tag{3}$$

which contains only three independent parameters α, β, and ζ. The reduction to a smaller number of parameters makes it much easier to analyze the Duffing oscillator.

An important feature of Eq. (3) is the $\pm$ sign in the linear force s. With a positive sign, the oscillator is always subject to a restoring force due to the positive linear and nonlinear stiffness. The potential energy is $U(s) = s^2/2 + \beta s^4/4$ and has a single minimum (single-well potential). When the sign is negative, we have a negative linear stiffness and a repelling linear force dominates for small amplitudes. The cubic restoring force dominates when the amplitude increases, maintaining the oscillations bounded. The potential energy in this case $U(s) = -s^2/2 + \beta s^4/4$ has two minima (double-well potential).

The Duffing oscillator has been widely investigated [10]. It is well known that it can develop a chaotic dynamics when excited by a single harmonic frequency for both single and double-well potentials [10]. In the last case, the system presents homoclinic chaos. The chaotic dynamics in this case is characterized by the switching between wells, which favors the appearance of chaos [1]. Therefore, for the double-well chaos is more easily found than in the single-well case. The chaotic regime has also been investigated experimentally and theoretically when the Duffing oscillator is excited by more than one harmonic frequency. The double-well Duffing oscillator (DWDO) excited by two frequencies was investigated experimentally by Moon and Holmes [22]. However, the experimental investigation took into account a limited region of the parameter space, in which no evidences of robust chaos were found. Soon after that, Wiggins [23] analyzed the DWDO theoretically and treating the effect of the superposed harmonic excitations as a perturbation was able to conclude that the threshold for chaos decreases significantly with the addition of a second harmonic excitation. Therefore, we should expect an increase in the regions where chaos is observed when the Duffing oscillator is excited by two frequencies. However, the result of Wiggins cannot be used to establish the size and shape of these regions, neither we can infer that the two-frequency excitation leads to robust chaos over a quite significant portion of the parameter space.

In fact, while for maps some strategies have been developed there is no general theoretical method to establish that a continuous time dynamical system presents robust chaos [8]. Due to the limitations of analytical methods, a purely numerical method for proving the existence of robust chaos was proposed by Gusso et al. [15]. The method consists in the search for the existence of more than one attractor (regular or chaotic) in a given region of the parameter space. For that purpose, the statistical moments of the attractors are calculated for a given set of parameters and for varying initial conditions (ICs). For chaos to be considered as robust, it is acceptable that these statistical moments vary only slowly as parameters are changed. For fixed parameters and different ICs, only small statistical fluctuations are acceptable. If the region in the parameter space is swept with sufficiently high resolution and a large number of ICs are tested for each point, it is proved that chaos is robust in the case that no data point is observed that differs significantly from its neighbors. This is a proof in the sense that the probability that chaos is *not* robust becomes negligible.

In what follows, we are going to study Eq. (3) with an added forcing term of the form $\cos(\zeta\tau/r)$, where $r > 1$ represents the ratio between the two excitation frequencies. While there is an effect of the amplitude of the second excitation, it is with equal amplitude that the

best results are obtained for the robustization of chaos, and we are going to present results only for this case. The resulting equation

$$\ddot{s} + \alpha\dot{s} \pm s + \beta s^3 = \cos(\zeta\tau) + \cos(\zeta\tau/r), \qquad (4)$$

is solved numerically using the method of Runge–Kutta of fourth and eighth order in Fortran and Wolfram's *Mathematica*, respectively. A transient corresponding to 3500 times the period of the fastest excitation is used. We have observed that this comparatively long transient time was necessary to assure only a negligible number of points with transient chaos in the final results. In what follows, chaos is characterized by the calculation of the maximum Lyapunov exponent, λ. Due to the low dissipations, we are going to consider the values of λ are of the order of $0.1 \sim 0.01$. Following Gusso et al. [15], where λ for the nanoresonator was of the same order, the dynamics is considered chaotic whenever $\lambda > 10^{-3}$, thus preventing the effects of small statistical fluctuations due to limited numerical precision.

3 Results for double-well potential

In the investigation of the nanoelectromechanical resonator by Gusso et al. [15], the magnitude of an applied voltage bias could be varied to produce a single- or double-well effective potential energy. While this potential was only a rough approximation in a system with strong parametric excitation, it was observed that the effect of chaotification produced by the second applied frequency was mostly concentrated in the double-well region. Therefore, we can expect that the robust chaotic dynamics is more likely to be found in the DWDO and we start by focusing on this case. However, we later investigate the single-well Duffing oscillator (SWDO) under two-frequency excitation which also presents interesting results.

3.1 Chaotification

The first step toward the proof that there is robust chaos in the DWDO is to investigate the regions in the parameter space where chaos is observed. For that purpose, we have calculated phase diagrams where the regions with periodic and chaotic attractors are distinguished.

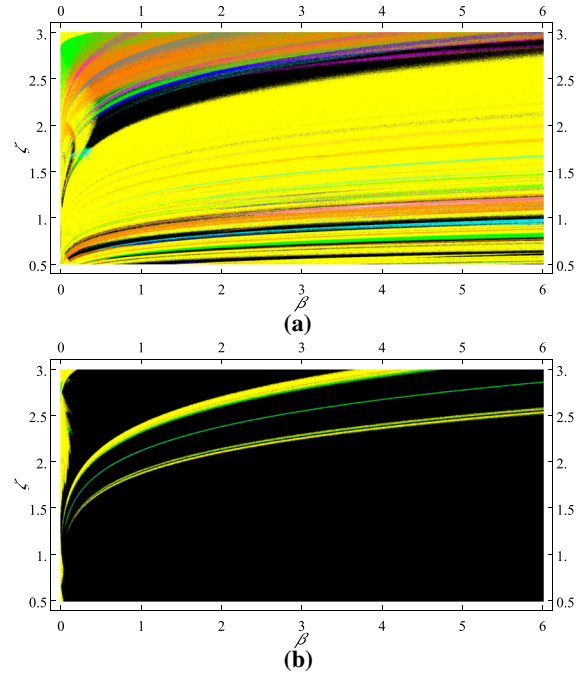

Fig. 1 Phase diagrams showing the regions with periodic and chaotic attractors. Results for the double-well Duffing oscillator with $\alpha = 0.01$ subject to **a** single excitation frequency and **b** two frequencies with $r = 1.07$. The color code is the following. For the periodic attractors: yellow (period 1—P1), green (P2), orange (P3), blue (P4), cyan (P5), magenta (P6), pink (P7), brown (P8). Periods above 8 are colored gray, and chaos is presented in black. The figures have a xy resolution of 2400×1000

To obtain the phase diagrams, two parameters are varied with high resolution, the nondimensional frequency ζ, and the nonlinearity β. Different phase diagrams have then been calculated for different values of dissipation α and the frequency ratio r. In all cases, the ICs were the same: $s(0) = v(0) = 0$.

In order to appreciate the relevance of the effect of the second harmonic excitation, in Fig. 1a we present the results for the system excited by a single frequency. In Fig. 1b, a second frequency respecting the ratio $r = 1.07$ is also exciting the DWDO. We can see that while for the single frequency (1f) excitation chaos is observed on small strips that traverse the region along the direction of the axis of the parameter β, for two-frequency (2f) excitation the opposite occurs and, in a region dominated by chaos, only thin strips of periodicity are observed. In spite of the high resolution of Fig. 1b, not a single point with periodicity is found within the black region below the lowest strip defining a periodic region. Therefore, with addition of the second fre-

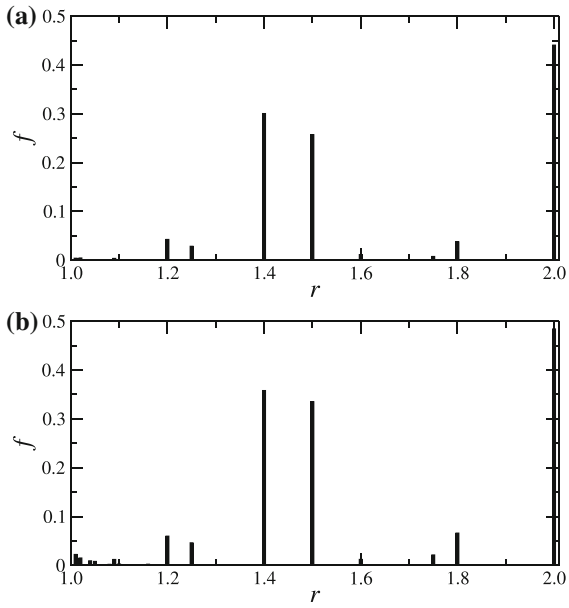

Fig. 2 Fraction f of periodic points within the region $\mathcal{A}$ defined by $\beta \in [2, 5]$ and $\zeta \in [1.0, 2.0]$ as a function of r with steps $\Delta r = 0.01$. In **a** $\alpha = 0.005$ and in **b** $\alpha = 0.01$

quency with an equal amplitude we have obtained an extreme chaotification of the dynamics. It is worth to note that for the periodic dynamics in Fig. 1b the period of the periodic attractors is not the same as those in Fig. 1a. While in (a) the periods of oscillation are multiples of $T = 2\pi/\zeta$, a period one attractor in (b) has a period that equals 107 times T. This occurs because the frequency ratio is a rational of the form $r = 107/100$, and the excitation is periodic with period $107 \times T$. In general, if we can represent the frequency ratio as the rational $r = m/n$, with $m, n \in \mathbb{N}^*$, the excitation is periodic with period $T_m = m \times T$ or, equivalently, $T_m = n \times rT$. Therefore, the strips of periodic behavior result from the locking of the DWDO with this periodic excitation.

This much extended fundamental period implies that considering the transient time, the total simulation time must be, at least, $(3500 + P \times m)T$, for probing period P ($P = 1, 2, 3 \ldots$) oscillations. As we have probed periods up to $P = 12$, the total simulation times can be rather large if we do not restrict m. For this reason in our analysis, we have chosen to take r between 1 and 2 with a resolution of 0.01. In this case, the largest m was 199. The use of such ratios suffices for our analysis since the chaotification of the DWDO does not depend so crucially on r. In particular, r does not need to be an irrational, what would be a stringent requirement for practical applications. To demonstrate how r can affect the chaotification, we investigate in more detail a particular region of the parameter space. Based on Fig. 1b, the region with $\beta \gtrsim 2$ and $\zeta \lesssim 2$ is free of points with periodicity. However, phase diagrams for other r have revealed that this large region with chaos can be either larger or smaller. We have thus sought an optimal region with chaos to investigate. A comparatively large region in the $\beta \times \zeta$ plane which still presented very low content of periodic points was the region $\mathcal{A}$ defined by $\beta \in [2, 5]$ and $\zeta \in [1, 2]$. Figure 2 presents the fraction f of periodic points within $\mathcal{A}$ as a function of r, which varied between 1.01 and 2 in steps of 0.01. The Lyapunov exponent for a total of 10.000 points, evenly distributed in the region, was calculated for each r and used to classify a point as periodic or chaotic. It can be seen that f in the region increases significantly only for some particular values of $r = m/n$ corresponding to the cases where both m and n are small integers, like $r(m/n) = 1.2(5/6), 1.25(5/4), 1.4(7/5), 1.5(3/2)$, and $1.8(9/5)$. This result is analogous to that found in [15] for the nanoresonator when a three parameter volume was also investigated in more detail for the relation between points with chaos and periodicity in its interior. Therefore, except for very specific frequencies, an extraordinary level of chaotification is obtained within a large region of the parameter space. We note that other regions of the parameter space have been investigated in this same way and similar results have been obtained. However, depending on the region chosen, particularly with ζ below 1, f becomes significant for a continuum of r values above $r \sim 1.4$.

The investigation of the nanoresonator by Gusso et al. [15] also revealed a crucial dependence of the chaotification with damping. We have also found a similar trend which is revealed in Fig. 3. For large dissipations, the effect of chaotification is reduced. Yet, below $\alpha \sim 0.02$ no periodic points have been observed down to $\alpha = 0.001$, the smallest value we considered. We have also investigated other values of r and different regions in the parameter space, and a similar trend was observed. However, it was possible to observe, for specific frequency ratios, the existence of large regions in the $\beta \times \zeta$ plane that did not present periodic points for α as large as 0.1.

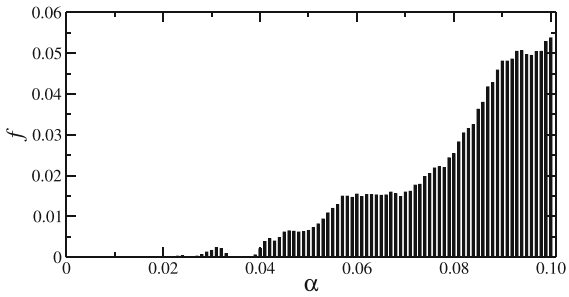

Fig. 3 Fraction f of periodic points within the region $\mathcal{A}$ obtained for $r = 1.07$ as a function of α, with steps $\Delta\alpha = 0.001$

3.1.1 Comparison with analytical predictions of chaos

We have observed that most of the parameter space in Fig. 1b has developed a chaotic dynamics under 2f-excitation. Interestingly, the existence of this large region was predicted theoretically. Generalizing the Melnikov's method Wiggins [23] was able to predict that for the Duffing oscillator excited by two frequencies chaos could exist if

$$\beta > \beta_l = \frac{8\alpha^2}{[\zeta\ \mathrm{sech}(\pi\zeta/2) + r^{-1}\zeta\ \mathrm{sech}(\pi r^{-1}\zeta/2)]^2}, \tag{5}$$

where β_l denotes the lowest required value of β. Taking $r = 0$ in this equation, we recover the usual prediction based on Melnikov's method for 1f-excitation [24]. This inequality sets a necessary, but not sufficient, condition for the existence of chaos. It has to be noted that the addition of a second frequency lowers the threshold for the existence of a chaotic dynamics. Considering $\alpha = 0.01$, as used in Fig. 1, Eq. (5) predicts that chaos can exist for rather low values of β. For the 2f-excitation with $r = 1.07$, for instance, β_l increases from $\sim 10^{-5}$ for $\zeta = 0.5$ to only $\sim 10^{-3}$ for $\zeta = 3$. For the 1f-excitation, these value are about three times larger, but still very small. In fact, they are so small that it is not worth showing the separatrix $\beta = \beta_l(\zeta)$ in Fig. 1.

While the vast majority of the region depicted in Fig. 1a, b satisfies the necessary condition for the existence of chaos, for 1f-excitation only a small fraction of the parameter space actually exhibits chaos. This is, in fact, the result commonly found in most systems for which chaos can be predicted based on Melnikov's method [24]. However, for the 2f-excitation almost

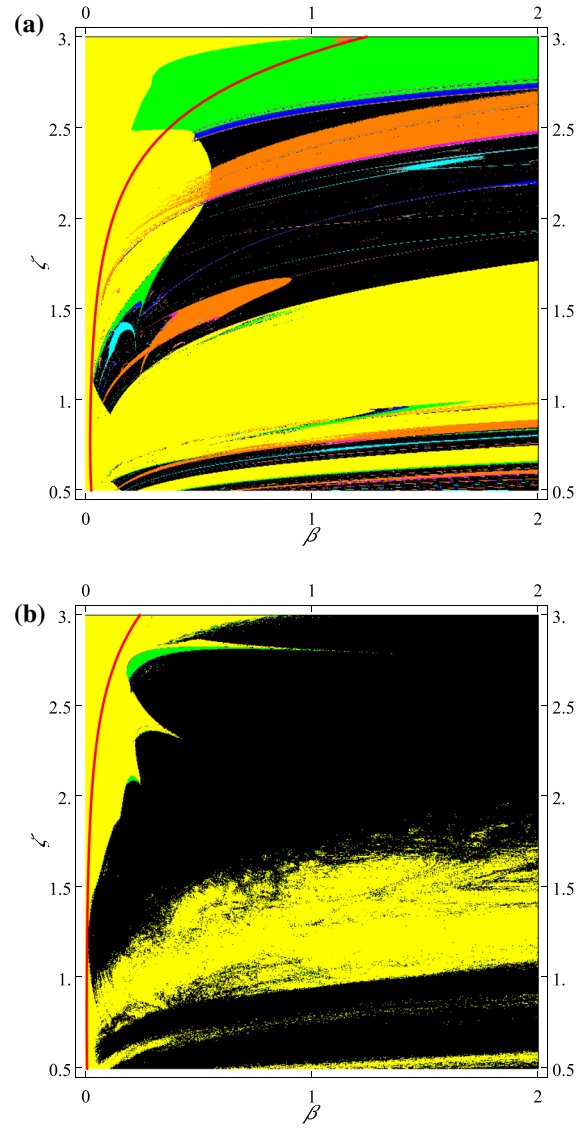

Fig. 4 Statistical moments obtained for 200 random ICs for points in the $\beta \times \zeta$ plane for the DWDO with $r = 1.07$ and $\alpha = 0.01$. The **a** dispersion and **b** kurtosis for s (v) are presented in red (black). A nonmonotonic and fast change of the statistical moments can be observed in this region of the parameters space, characterized by smaller ζ

all this region has developed a chaotic dynamics for $\alpha = 0.01$. The interesting prediction by Wiggins [23] that the 2f-excitation lowers the threshold for the emergence of chaos is evidenced in Fig. 4, where a larger α, equal to 0.2, is used allowing to trace the separatrix $\beta = \beta_l(\zeta)$. Comparing both panels in Fig. 4, it is clear that chaos indeed emerges for values of β not allowed for the 1f-excitation.

3.2 Robust chaos

The existence of a significant region continuously covered with points with chaos in the parameter space is a necessary but not sufficient condition for the existence of robust chaos. Ideally, the observed vast chaotification in the parameter space should be due to a single chaotic attractor for chaos to be robust. However, except for certain maps, the attractor of dynamical systems varies as parameters are changed. This was the case, for instance, in the first map with robust chaos analyzed by Banerjee et al. [12]. Therefore, the requirement that the attractor does not change is relaxed and what is usually required, instead, is only that the attractor be locally robust. That means small changes in the system parameters do not significantly change the attractor. As a consequence, for large variations of the parameters, what is require is that the attractor varies slowly.

Because of the lack of sufficiently general analytical methods for proving that a dynamical systems present robust chaos, in [15] a formal numerical method was proposed and used for that purpose. The proof is based in the following three conditions that must be satisfied simultaneously over a region of the parameter space: (i) contiguous points in a high-resolution grid in the relevant parameter space evolve toward a chaotic attractor (the system is not attracted to either periodic or quasi-periodic orbits); (ii) at each grid point, the chaotic attractor must be unique; and (iii) the statistical properties used to describe the chaotic attractor change slowly and smoothly along the grid. Conditions (i) and (ii) are necessary to determine that chaotic attractor is unique within the region being considered, while condition (iii) is introduced to ensure that the attractor persists (does not change significantly) under small changes of the parameters. Following this method, we proved that there are large regions with robust chaos for the Duffing oscillator excited by two frequencies.

In order to characterize all possible attractors that may exist at each point of the grid in the parameter space and for different ICs, we calculate the first four statistical moments for each dynamical variable, in this case s and $v = \dot{s}$. More specifically, for s we calculate the mean, dispersion, skewness, and kurtosis, respectively, given by

$$\bar{s} = \frac{1}{N}\sum_{i=1}^{N} s_i,$$

$$\delta s = \sqrt{\frac{\sum_{i=1}^{N}(s_i - \bar{s})^2}{N}}$$

$$\gamma s = \frac{1}{N}\frac{\sum_{i=1}^{N}(s_i - \bar{s})^3}{\delta s^3},$$

$$\kappa s = \frac{1}{N}\frac{\sum_{i=1}^{N}(s_i - \bar{s})^4}{\delta s^4}, \quad (6)$$

with similar expressions for v. We expect that any two distinct attractors have, at least, one of these eight statistical quantities with significantly different values. That is the case for all systems with multiple attractors known by the authors.

We have performed the analysis presented above in most of the area that is below the lowest strip of periodicity seen in Fig. 1b. We present first the results that demonstrate the existence of a large area with robust chaos which corresponds to region $\mathcal{A}$. We have checked if the chaotification observed in Fig. 1b persists if the ICs are changed. For that purpose, a grid of points was created in $\mathcal{A}$ with a resolution of 0.025 in both β and ζ, resulting in a total of 4,800 points in the region. At each point, we solved Eq. (4) for 200 distinct and randomly chosen ICs which were taken within the ranges $s(0) \in [-3, 3]$ and $v(0) \in [-5, 5]$. This range of ICs was chosen because it defines a region in the phase space that encompasses the observed chaotic attractors. The s_i and v_i used to calculate the statistical moments of the attractor were obtained from the numerical solution of Eq. (4) for a total simulation time corresponding 150 times the period T_m beyond the transient. The points used to calculate the moments were sampled at a rate of $T_m/160$, resulting in $N = 24,000$.

In Fig. 5, we present the four statistical moments for the DWDO excited by frequencies with $r = 1.07$ and for $\alpha = 0.01$. Each of the 200 distinct results obtained for the different ICs are shown for each point in the $\beta \times \zeta$ plane. We can see that the 200 values obtained for the statistical moments resulting from each random IC are all closely clustered around a central value. For the mean and skewness, they are very close to zero. It is only for the kurtosis that a slightly larger dispersion is seen. It is, however, the result of the sensitivity of the higher order moment to fine details of the attractor, which are expected to have the same statistical properties only for an infinitely long sampling time. This clustering is an evidence that the chaotic attractor at each point in the grid is unique. Another feature of the results is the smooth variation of the points as β and ζ are changed. Actually, the variation occurs only for the

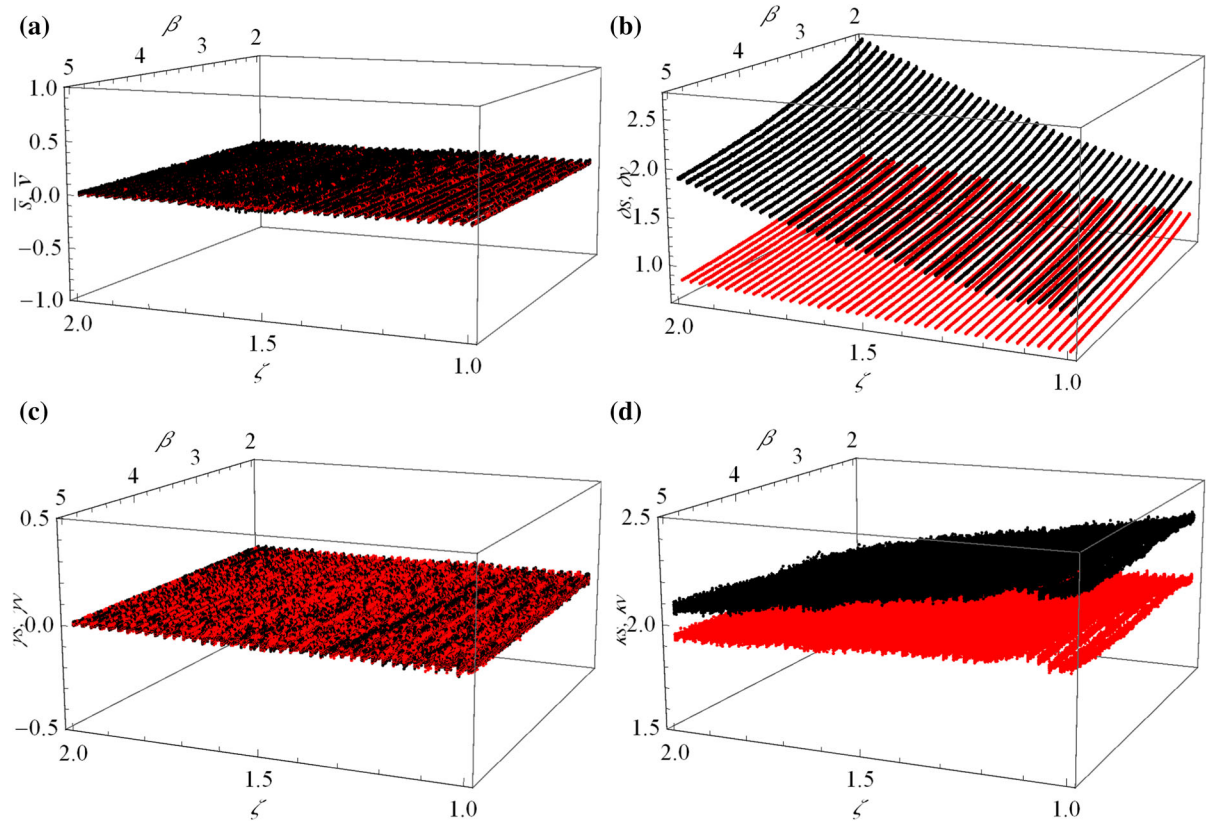

Fig. 5 Statistical moments obtained for 200 random ICs for points in the $\beta \times \zeta$ plane for the DWDO with $r = 1.07$ and $\alpha = 0.01$. The moments for s (v) are presented in red (black)

dispersion and the kurtosis, while the mean and skewness remain close to zero. The smooth variation is an evidence of the robustness of the chaotic attractor as mentioned previously.

We have performed the same analysis of the statistical moments for other ratios r and dampings α. The most noticeable difference with respect to the results already shown for region $\mathcal{A}$ was observed for ζ smaller than 1. This is illustrated in Fig. 6, where the dispersion and the kurtosis in a region with $\zeta \in [0.5, 1]$ clearly display fast changes for $\zeta \sim 0.7$. Therefore, in this region, the chaotic attractor may change significantly with small changes of the parameters, with a particular sensitivity to ζ, and criterion (iii) for chaos to be robust is not satisfied.

4 Results for single-well potential

While in an extension or the work in [15] the authors have observed for the nanoelectromechanical resonator the existence of regions with chaos that extended continuously from the region with an effective double-well potential to the one with a single-well, the robustness of the chaotic dynamics was proved in [15] only in a region with the double-well potential. However, it is interesting to know the effects of the 2f-excitation on the SWDO, because many physical systems are more frequently modeled as a SWDO than as a DWDO.

We have observed that the 2f-excitation also induces a significant chaotification in the SWDO. This is illustrated in Fig. 7 where the phase diagrams for the 1f and 2f-excitation for $r = 1.07$ and $\alpha = 0.01$ are presented. For 1f-excitation, only periodic attractors are seen in the region investigated, and when the second frequency is added a quite significant chaotification takes place. However, it is not so effective as for the DWDO. The region with chaos, observed at larger β, now contains a significant fraction of periodic attractors, distributed in disconnected pieces along this region. In such a case, it is difficult to use the SWDO as a reliable source

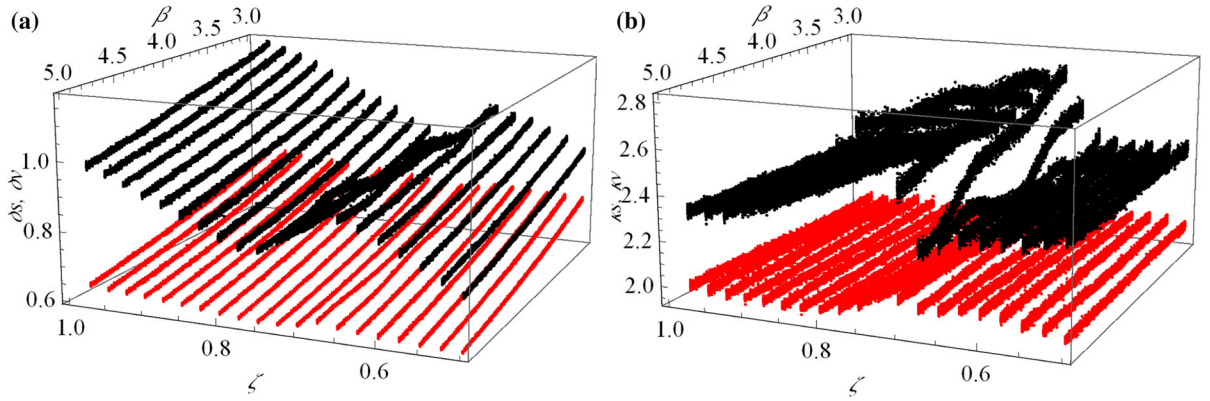

Fig. 6 Phase diagrams showing the regions with periodic and chaotic attractors for the double-well Duffing oscillator with $\alpha = 0.2$ subject to **a** single excitation frequency and **b** two frequencies with $r = 1.07$. The red curve separates the regions where chaos is possible or not according to Eq. (5). The color code is the same as that in Fig. 1. (Color figure online)

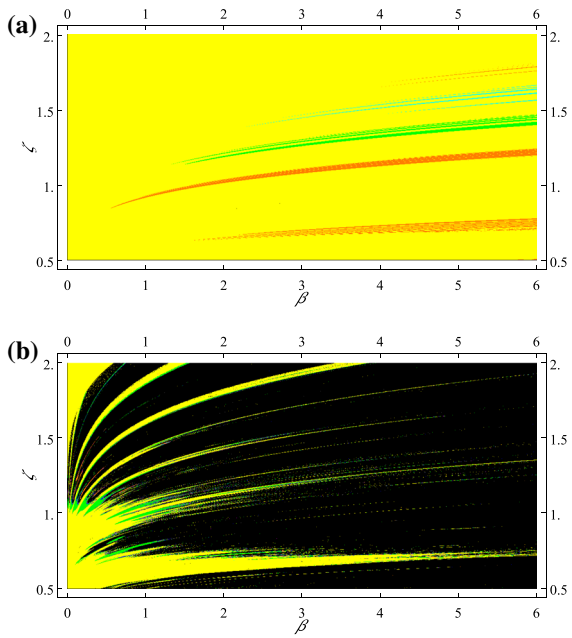

Fig. 7 Phase diagrams showing the regions with periodic and chaotic attractors for the single-well Duffing oscillator with $\alpha = 0.01$ subject to **a** single excitation frequency and **b** two frequencies with $r = 1.07$. The color code is the same as that in Fig. 1

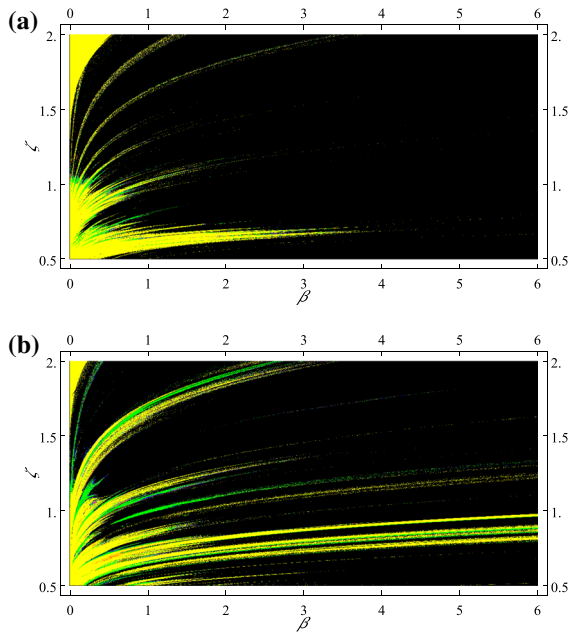

Fig. 8 Phase diagrams showing the regions with periodic and chaotic attractors for the single-well Duffing oscillator with $\alpha = 0.002$ subject to 2f-excitation. In **a** $r = 1.07$ and in **b** $r = 1.27$. The color code is the same as that in Fig. 1

of chaos. The presence of periodic attractors can be made smaller by the reduction in damping. In Fig. 8, α was reduced to 0.002, and for $r = 1.07$ a much better chaotification can be seen. While the chaotification is generally better for smaller dissipation, for certain frequencies the improvement is not so effective. This is illustrated by the result for $r = 1.27$ in Fig. 8b.

The chaotification in the SWDO is not only less effective, but the chaotic attractor is not robust along most of the region where chaos prevails. This conclusion can be drawn from the results in Fig. 9 for the dis-

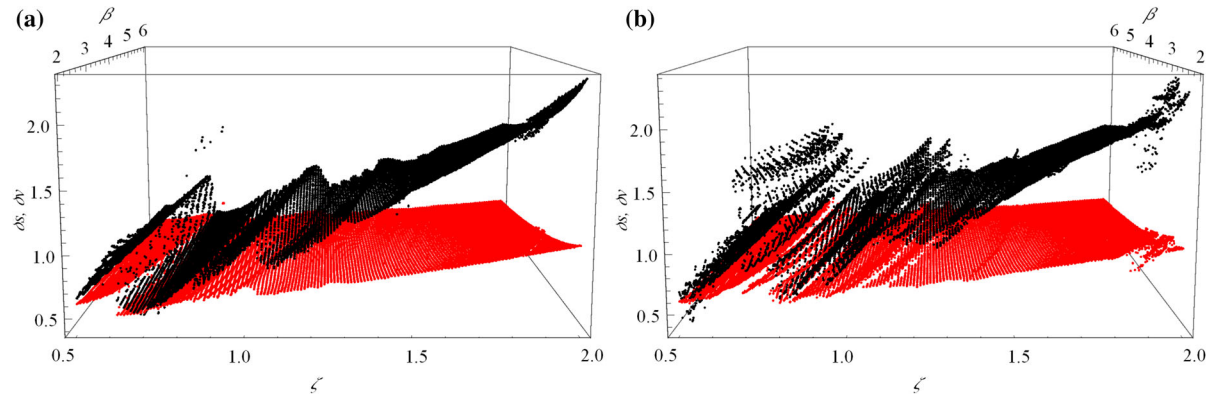

Fig. 9 The dispersion of the attractors for points in the $\beta \times \zeta$ plane for the SWDO with $\alpha = 0.002$ and **a** $r = 1.07$ and **b** $r = 1.27$. The dispersion for s (v) is presented in red (black)

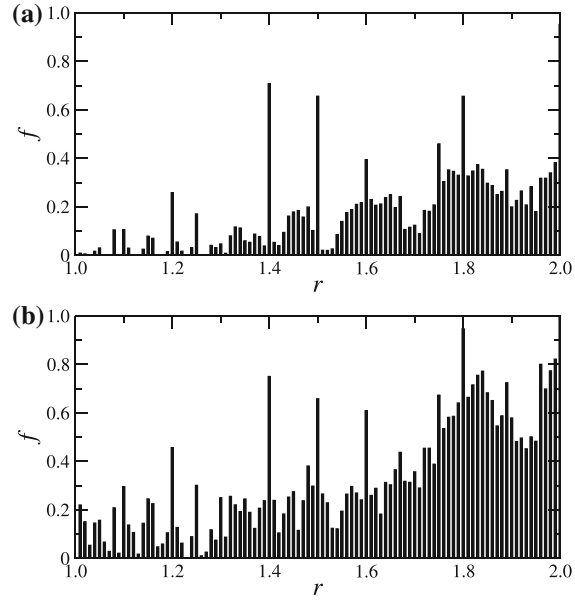

Fig. 10 Fraction f of periodic points within the region $\mathcal{C}$ defined by $\beta \in [3, 6]$ and $\zeta \in [1.5, 2.0]$ as a function of r with steps $\Delta r = 0.01$. In **a** $\alpha = 0.002$ and in **b** $\alpha = 0.01$

persion of the attractors in the $\beta \times \zeta$ plane, obtained for the same IC: $s(0) = v(0) = 0$. We display the results for a large region $\mathcal{B}$ on the parameter space that contains both the periodic and chaotic attractors and is defined by $\beta \in [2, 6]$ and $\zeta \in [0.5, 2]$. As both chaotic and periodic attractors coexist in the region investigated, we could expect the sudden changes in the statistical moments that are observed. However, what it is seen is that even in the regions with chaos the dispersion also changes significantly. While for $r = 1.07$, the variations of δs and δv may not seen so severe, for $r = 1.27$, for instance, sudden and almost random changes take place. It is only for ζ approximately between 1.5 and 2 that there seems to be a region with a smooth variation of the attractor and, possibly, robust chaos. We have further investigated the behavior of the attractors in $\mathcal{B}$ and by varying the ICs little has changed. Therefore, we conclude the chaotic attractor is unique at most of the points in $\mathcal{B}$, satisfying one of the criteria for chaos to be robust. However, condition (iii) established in Sect. 3.2 is not satisfied.

The small region where the statistical properties of the chaotic attractor are varying more regularly was investigated more carefully to check for the existence of robust chaos. Focusing on the region $\mathcal{C}$ defined by $\beta \in [3, 6]$ and $\zeta \in [1.5, 2]$ the ratio r was varied, and the fraction f of periodic points was calculated for different values of α. The results are shown in Fig. 10. It can be seen that for $\alpha = 0.01$ a significant fraction of periodic points exist for almost any r and it is generally much larger than for the DWDO. For lower dissipation $\alpha = 0.002$ f decreases for small r, but f is still significant for several r in this region. The result is even more disappointing if we note that the area of region $\mathcal{C}$ is only half that of $\mathcal{A}$. Even if region $\mathcal{C}$ is divided into two halves, the results within each half is quite similar to the whole area $\mathcal{C}$. The effect of the dissipation is also quite different in the case of the SWDO. In Fig. 11, we can see that only for very small dissipation, $\alpha \lesssim 0.003$, no periodic points are observed in $\mathcal{C}$ for the ratio $r = 1.07$. Above that there is a steady increase of f which is, at least, one order of magnitude larger than f for the DWDO for similar dissipation.

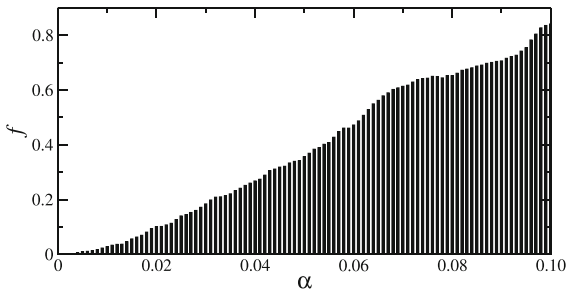

Fig. 11 Fraction f of periodic points within the region $\mathcal{C}$ obtained for $r = 1.07$ as a function of α, with steps $\Delta\alpha = 0.001$

Therefore, while we can conclude that the 2f-excitation can create small regions in the parameter space with robust chaos in the SWDO, this effect is much more limited, and more restricted in terms of acceptable frequency ratios and dissipation.

However, while the significant chaotification that we observe may not suffice for the use of the SWDO in practical applications, this phenomenon is relevant because chaos may emerge in several dynamical systems, modeled as a SWDO, much more easily then previously thought. In fact, chaos is hardly observed in the SWDO under 1f-excitation. It emerges only when the linear restoring force is negligible compared with that of the cubic nonlinearity. We have found through numerical simulations that, typically, a β larger than 200 is required to produce chaos. For such large β, the Duffing equation reduces to the famous pure cubic oscillator first investigated by Ueda [10,25].

The Ueda's oscillator presents a characteristic chaotic attractor in the phase portrait which displays two lobes that partially superimpose. A representative example of this attractor is displayed in Fig. 12a. In the case of 2f-excitation, we have also observed seemingly analogous chaotic attractors, in spite of the fact that they are obtained for β smaller by two orders of magnitude. As seen in the phase portrait in Fig. 12b, the two lobes are also present in this case. However, a set of circular trajectories are also seen around the origin of the phase space. The trajectories are likely due to the role played by the linear restoring force, which is of the same order as the cubic one. Also, when we compare the time series obtained for 1f and 2f-excitation, there are clear differences. In particular, for 2f-excitation the oscillations within the lobes (corresponding to the laminar states in the time series) are suppressed, while they prevail for the 1f-excitation. This change contrasts to what we observed in the DWDO, for which similar phase portraits and time series for both 1f and 2f-excitations are found. The distinctive dynamics of the SWDO under 2f-excitation certainly deserves further investigation. It represents a new chaotic regime in a system whose chaotic dynamics was extensively investigated in the literature [10,25] neglecting the role of the linear restoring force.

5 Conclusions

The results in Figs. 2 and 3 demonstrate that the 2f-excitation induces full chaotification of the DWDO over a quite significant portion of the parameter space, region $\mathcal{A}$, for a wide range of frequency ratios and when the dissipation is sufficiently small. In fact, only certain

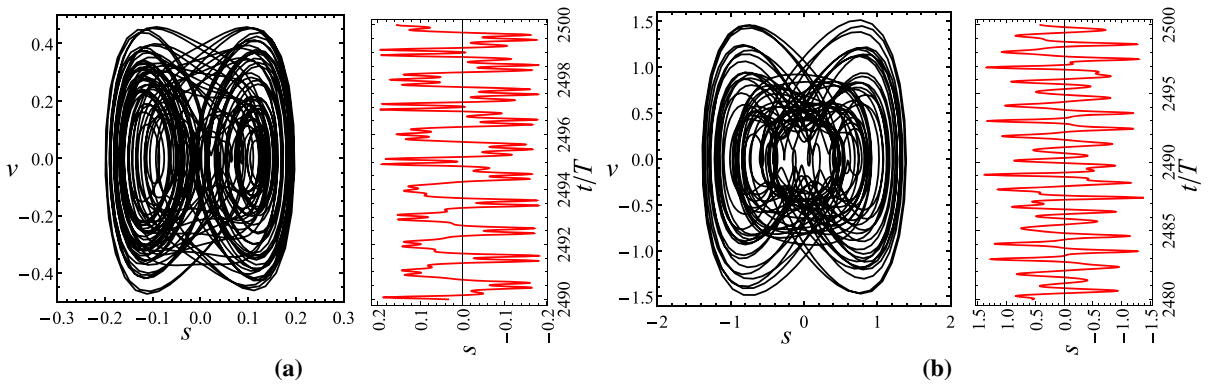

Fig. 12 Phase portraits and times series for **a** 1f-excitation and $\alpha = 0.01$, $\beta = 480$, $\zeta = 0.8$ and **b** 2f-excitation with $r = 1.27$ and $\alpha = 0.01$, $\beta = 1.7$, and $\zeta = 0.8$. The period T corresponds to $2\pi/\zeta$

very specific frequency ratios must be avoided. For the different values of r, we have tested in our investigations, which did not coincide with those that must be avoided, the behavior of the chaotic attractor is essentially that presented in Fig. 4 for $r = 1.07$. These results support the conclusion that chaos is robust within, at least, region $\mathcal{A}$.

The existence of a large region in the parameter space with robust chaos is important for the potential practical applications of the system. For instance, an electronic circuit designed to work as a source of chaos is going to be built with components that have certain fabrication tolerances. That is the case for either bulk components or those constructed in a microchip. The existence of a large region with robust chaos allows for larger design tolerances, since the system parameters can vary, but the existence of a chaotic dynamics with statistical properties close to that of the design is assured. The high tolerance to changes in the system parameters also makes the DWDO under 2f-excitation less sensitive to external perturbations and the changes that occur due to the aging of components.

Applications that rely upon the change of parameters of the system can also benefit. For instance, the robustness of the chaotic dynamics must allow the use of larger perturbations of the system parameters to encode signals, rather than the small perturbations used in chaotic modulation schemes [26].

Despite the significant chaotification predicted for the SWDO, we have seen that no sufficiently large areas with robust chaos could be found in the parameter space that support the system as an adequate source of chaotic signal. However, the result indicates that chaos can emerge much more easily in many systems whose dynamics is dictated by the single well Duffing equation. This can occur even for system with significant damping. Therefore, the design and analysis of any physical system that can be, at least approximately, modeled as a SWDO and is subject to more than a single excitation frequency, should take into account that chaos could be part of its dynamics. This need becomes more evident from the comparison of the results in Fig. 7 for the 1f and 2f-excitation of the SWDO.

Due to the existence of both beneficial and detrimental consequences of a strong chaotification by 2f-excitation, further investigations are needed. It is important to know if other systems besides the suspended beam micro- and nanoresonators [15] and the Duffing oscillator suffer a strong chaotification and can present robust chaos. In particular, it would be interesting to know what other system may develop robust chaos, due to the potential relevance for practical applications. Finally, while there is no general theory or method to establish if a system presents robust chaos its important to pursue an adequate theoretical explanation to why robust chaos emerges in these systems.

Acknowledgements R. L. Viana was supported by the National Research Funding Agency, CNPq-Brasil, Grant 301019/2019-3.

Compliance with ethical standards

Conflict of interest The authors declare that they have no conflict of interest.

References

1. Strogatz, S.H.: Nonlinear Dynamics and Chaos: With Applications to Physics, Biology, Chemistry, and Engineering. Westview Press, Boulder (2015)
2. Cuomo, K.M., Oppenheim, A.V.: Circuit implementation of synchronized chaos with applications to communications. Phys. Rev. Lett. **71**, 65–68 (1993)
3. Kocarev, L.: Chaos-based cryptography: a brief overview. IEEE Circuits Syst. Mag. **1**, 6–21 (2001)
4. Verschaffelta, G., Khoder, M., Van der Sande, G.: Random number generator based on an integrated laser with on-chip optical feedback. Chaos **27**, 114310 (2017)
5. Dantas, W.G., Rodrigues, L.R., Ujevic, S., Gusso, A.: Using nanoresonators with robust chaos as hardware random number generators. Chaos **30**, 043126 (2020)
6. Deane, J.H.B., Hamill, D.C.: Improvement of power supply EMC by chaos. Electron. Lett. **32**, 1045 (1996)
7. Carroll, T.L., Rachford, F.J.: Target recognition using nonlinear dynamics. In: Leung, H. (ed.) Chaotic Signal Processing, pp. 23–48. SIAM, Philadelphia (2013)
8. Zeraoulia, E., Sprott, J.C.: Robust Chaos and Its Applications. World Scientific Publishing, Singapore (2012)
9. Zhang, H., Liu, D., Wang, Z.: Controlling Chaos. Springer, London (2009)
10. Kovacic, I., Brennan, M.J.: The Duffing Equation Nonlinear Oscillators and Their Behavior. Wiley, London (2011)
11. Gallas, J.: The structure of infinite periodic and chaotic hub cascades in phase diagrams of simple autonomous flows. Int. J. Bifurc. Chaos **20**, 197–211 (2010)
12. Banerjee, S., Yorke, J.A., Grebogi, C.: Robust chaos. Phys. Rev. Lett. **80**, 3049–3052 (1998)
13. Kuznetsov, S.P., Seleznev, E.P.: A strange attractor of the Smale–Williams type in the chaotic dynamics of a physical system. J. Exp. Theor. Phys. **102**, 355–364 (2006)
14. Isaeva, O.B., Kuznetsov, S.P., Sataev, I.R., Savin, D.V., Seleznev, E.P.: Hyperbolic chaos and other phenomena of complex dynamics depending on parameters in a nonautonomous system of two alternately activated oscillators. Int. J. Bifurc. Chaos **25**, 1530033 (2015)

15. Gusso, A., Dantas, W.G., Ujevic, S.: Prediction of robust chaos in micro and nanoresonators under two-frequency excitation. Chaos **29**, 033112 (2019)
16. Wang, Y.C., Adams, S.G., Thorp, J.S., MacDonald, N.C., Hartwell, P., Bertsch, F.: Chaos in MEMS, parameter estimation and its potential application. IEEE Trans. Circuits Syst. **I**(45), 1013–1020 (1998)
17. DeMartini, B.E., Butterfield, H.E., Moehlis, J., Turner, K.L.: Chaos for a microelectromechanical oscillator governed by the nonlinear Mathieu equation. J. Microelectromech. Syst. **16**, 1314–1323 (2007)
18. Barceló, J., de Paúl, I., Bota, S., Segura, J., Verd J.: Chaotic signal generation in the MHz range with a monolithic CMOS-MEMS microbeam resonator. In: 2019 IEEE 32nd International Conference on Micro Electro Mechanical Systems (MEMS), pp. 1037–1040 (2019). https://doi.org/10.1109/MEMSYS.2019.8870887
19. Cleland, A.N.: Foundations of Nanomechanics. Springer, Berlin (2003)
20. Younis, M.I.: MEMS Linear and Nonlinear Statics and Dynamics. Springer, New York (2011)
21. Tamaseviciute, E., Tamasevicius, A., Mykolaitis, G., Bumeliene, S., Lindberg, E.: Analogue electrical circuit for simulation of the Duffing–Holmes equation. Nonlinear Anal. Model **13**, 241–252 (2008)
22. Moon, F.C., Holmes, W.T.: Double Poincaré sections of a quasiperiodically forced chaotic attractor. Phys. Lett. A **111**, 157–160 (1985)
23. Wiggins, S.: Chaos in quasiperiodically forced Duffing oscillator. Phys. Lett. B **124**, 138–142 (1987)
24. Guckenheimer, J., Holmes, P.: Nonlinear Oscillations, Dynamical Systems, and Bifurcations of Vector Fields. Springer, New York (1983)
25. Ueda, Y.: Random phenomena resulting from nonlinearity in the system described by Duffing's equation. Int. J. Non-Linear Mech. **20**, 481–491 (1985)
26. Yang, T., Chua, L.: Secure communication via chaotic parameter modulation. IEEE Trans. Circuit. Syst. -I **43**, 817–819 (1996)